

Pessimistic Iterative Planning for Robust POMDPs

Maris F. L. Galesloot¹ Marnix Suilen¹ Thiago D. Simão² Steven Carr³
Matthijs T. J. Spaan⁴ Ufuk Topcu³ Nils Jansen^{1,5}

¹Radboud University Nijmegen ²Eindhoven University of Technology

³University of Texas at Austin ⁴Delft University of Technology ⁵Ruhr-University Bochum

ABSTRACT

Robust POMDPs extend classical POMDPs to handle model uncertainty. Specifically, robust POMDPs exhibit so-called *uncertainty sets* on the transition and observation models, effectively defining ranges of probabilities. Policies for robust POMDPs must be (1) memory-based to account for partial observability and (2) robust against model uncertainty to account for the worst-case instances from the uncertainty sets. To compute such robust memory-based policies, we propose the *pessimistic iterative planning* (PIP) framework, which alternates between two main steps: (1) selecting a *pessimistic* (non-robust) POMDP via worst-case probability instances from the uncertainty sets; and (2) computing a finite-state controller (FSC) for this pessimistic POMDP. We evaluate the performance of this FSC on the original robust POMDP and use this evaluation in step (1) to select the next pessimistic POMDP. Within PIP, we propose the *RFSCNET* algorithm. In each iteration, *RFSCNET* finds an FSC through a recurrent neural network by using *supervision policies* optimized for the pessimistic POMDP. The empirical evaluation in four benchmark environments showcases improved robustness against several baseline methods and competitive performance compared to a state-of-the-art robust POMDP solver.

KEYWORDS

Robust POMDPs, Finite-State Controllers, Recurrent Neural Networks

1 INTRODUCTION

Partially observable Markov decision processes [POMDPs; 36] are the standard model for decision-making under uncertainty. *Policies* select actions based on limited state information towards some objective, for instance, minimizing the expected cost. Optimizing policies for POMDPs is extensively studied [3, 22, 42, 60, 66].

Policies for POMDPs. Policies inherently depend on the sequences of past actions and observations, also known as the *history*. That is, the policies require *memory*, which can be represented by recurrent neural networks (RNNs) or finite-state controllers (FSCs).

RNNs represent memory-based policies [52] thanks to their ability to learn sufficient statistics of the history [44]. RNNs have successfully been used in POMDPs within reinforcement learning [5, 23, 25] and planning [12]. However, computing the expected performance of an RNN policy relies on simulations and cannot be done analytically, hindering a proper policy evaluation.

FSCs offer a more structured way to represent policies and, given the POMDP model, allow a precise and efficient numerical evaluation of their performance [48]. However, finding FSCs often relies on selecting a predetermined memory size and structure [35]. An

exhaustive search for the optimal size and structure may, in general, be computationally intractable.

Drawing from the benefits of both representations, Carr et al. [12] extract the memory structures for FSCs from RNNs that are trained on data collected from the POMDP. Consequently, the exact memory structure need not be specified a-priori, and one may determine the FSC’s memory size flexibly.

Robust POMDPs and policies. A standard assumption in POMDPs is that probabilities are precisely known for the transition and observation functions of a POMDP. This assumption is unrealistic, for example, when probabilities are derived from historical data, sensors with limited precision, or domain experts expressing uncertainty [37, 71]. *Robust POMDPs* [RPOMDPs; 57] overcome this assumption by introducing *uncertainty sets*, i.e., sets of probabilistic transition and observation functions. *Robust policies* account for this uncertainty *pessimistically*, that is, they optimize against the *worst-case* instances within the uncertainty sets. Consequently, a robust policy provides a lower bound on its actual performance. Altogether, robust policies for RPOMDPs must be (1) memory-based to deal with limited state information and (2) pessimistically account for uncertainty. This paper aims to compute such robust memory-based policies for RPOMDPs.

FSCs representing robust policies. The first step is to discuss a proper representation of robust policies. As these policies must be optimized against the worst-case instance of the uncertainty sets, determining this exact worst-case is paramount. For FSCs, we can perform *robust policy evaluation* in RPOMDPs through robust dynamic programming [32, 54]. In particular, we can determine the exact worst-case probabilities to evaluate the FSC’s performance. Finding robust policies represented as FSCs, however, suffers from the same problems as in POMDPs, that is, selecting a predetermined memory size and structure, as done in *sequential convex programming* [SCP; 17]. As our empirical evaluation shows, specifying more memory may lead to worse results for SCP in RPOMDPs since, apart from an increase in the complexity of numerical evaluation, the memory size affects the number of variables to be optimized.

Contributions

We propose a general framework for robust memory-based planning in RPOMDPs, as outlined in Figure 1, and within this framework, an algorithm that combines the representational power of RNNs and the exact robust evaluation of FSCs.

Pessimistic iterative planning for RPOMDPs (Section 4). We propose the *pessimistic iterative planning* (PIP) framework to find a robust policy for RPOMDPs. PIP computes policies for POMDPs within the uncertainty sets of the RPOMDP that are *pessimistic* instances to the current policy, i.e., a worst-case instance given the

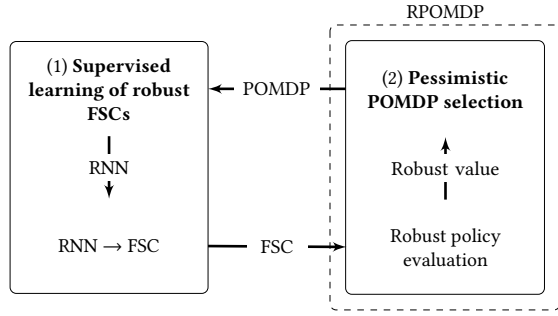


Figure 1: Overview of the PIP framework. The steps generating an FSC for pessimistic POMDPs on the left are specific to rFSCNET. The steps on the right are generally applicable.

current policy. PIP alternates between two main steps: (1) computing FSCs for (pessimistic) POMDPs and (2) evaluating the FSC on the RPOMDP and selecting pessimistic POMDPs. We implement PIP in our RNN-based algorithm, named rFSCNET, which consists of the following two main parts, corresponding to the steps of PIP:

- (1) **Supervised learning of robust FSCs** (Section 5). We train an RNN based on data collected from *supervision policies* that we optimize for the pessimistic POMDPs. From the RNN, we extract the FSC that we use for robust policy evaluation and pessimistic POMDP selection. With these pessimistic POMDPs, we further train the RNN by refining the collected histories and associated supervision policy, guiding the RNN and, therefore, the extracted FSCs towards a robust policy.
- (2) **Pessimistic POMDP selection** (Section 6). First, we compute the worst-case performance of the FSC on the RPOMDP via robust policy evaluation, thereby producing a guaranteed lower bound on its performance. Using the results from the FSC’s robust evaluation, we construct a linear program that efficiently finds a POMDP instance within the uncertainty sets that is pessimistic, *i.e.*, a worst-case, to the current FSC.

In our experimental evaluation on four benchmarks, we (1) show-case that the FSCs found by our method are competitive with and outperform the state-of-the-art FSC-based solver for RPOMDPs by Cubuktepe et al. [17], and, (2) conduct an ablation study to show the impact of our contributions on robustness, namely iteratively finding and re-training on pessimistic POMDPs, as opposed to baselines that train on either fixed or random POMDPs within the uncertainty set of the RPOMDP.

2 PRELIMINARIES

The set of all probability distributions over X is denoted by $\Delta(X)$. A distribution $\mu \in \Delta(X)$ is called *Dirac* if $\mu(x) = 1$ for precisely one $x \in X$ and zero otherwise. The number of elements in a set X is denoted by $|X|$. *Iverson brackets* return $[P] = 1$ if predicate P is true and 0 otherwise. Finally, the set of *probability intervals* with lower bounds strictly greater than zero is $\mathbb{I} = \{[i, j] \mid 0 < i \leq j \leq 1\}$.

DEFINITION 1 (POMDP). A partially observable Markov decision process is a tuple $M = \langle S, A, T, Z, O, C \rangle$, where S, A, Z are finite

sets of states, actions, and observations, $T: S \times A \rightarrow \Delta(S)$ is the probabilistic transition function, $O: S \rightarrow Z$ is the deterministic state-based observation function, and $C: S \times A \rightarrow \mathbb{R}_{\geq 0}$ is the bounded cost (or reward) function.

For simplicity and without loss of generality, we consider POMDPs with *deterministic* observations, where the observation function maps only to Dirac distributions. This assumption is non-restrictive as every POMDP can be transformed into one with deterministic observations [15, Remark 1].

A *trajectory* in a POMDP is a (in)finite sequence of states and actions: $\omega_H = s_1 a_1 s_2 \dots s_H \in (S \times A)^{H-1} \times S$, such that $T(s_{t+1} \mid s_t, a_t) > 0$ for $1 \leq t < H$. A *history* is the observable fragment of a trajectory: $h_H = O(s_1) a_1 O(s_2) \dots O(s_H) = z_1 a_1 z_2 \dots z_H \in (Z \times A)^{H-1} \times Z$. The set of all (finite) trajectories and associated histories are Ω and \mathcal{H} , respectively. Histories can be compressed into sufficient statistics known as *beliefs*, that is, probability distributions over states [36]. The set of all beliefs in a POMDP is $\mathcal{B} \subseteq \Delta(S)$. The initial state distribution (belief) is $b_0 \in \mathcal{B}$. A belief $b \in \mathcal{B}$ can be computed from a history $h \in \mathcal{H}$ using Bayes’ rule [67].

A *Markov decision process* (MDP) is a POMDP where each state is fully observable, and a *Markov chain* (MC) with rewards, also known as a *Markov reward process*, is an MDP with a single action, which can be omitted [61].

2.1 Policy Representations and Expected Costs

A *policy* resolves the action choices in a POMDP and is a function $\pi: \mathcal{H} \rightarrow \Delta(A)$ that maps histories to distributions over actions. Since beliefs are sufficient statistics for histories, policies may also be belief-based, *i.e.*, of type $\pi: \mathcal{B} \rightarrow \Delta(A)$. A policy is deterministic if it only maps to Dirac distributions, and the set of all (history-based) policies is denoted by Π .

We seek to find a policy $\pi \in \Pi$ that minimizes the expected cost of reaching goal states $G \subseteq S$, also known as the stochastic shortest path (SSP) problem [6]. For any trajectory ω , the cumulative cost $\rho_{\diamond G}: \Omega \rightarrow \mathbb{R}_{\geq 0} \cup \{+\infty\}$ is [18]:

$$\rho_{\diamond G}(\omega) = \begin{cases} \infty & \forall t \in \mathbb{N}, s_t \notin G, \\ \sum_{t=0}^{\min\{t \mid s_t \in G\}-1} C(s_t, a_t) & \text{otherwise.} \end{cases} \quad (1)$$

The SSP objective is to find an optimal policy $\pi \in \Pi$ that minimizes the *expected cumulative cost* J_T^π of the trajectories generated under policy π and transition function T :

$$\pi^* \in \operatorname{argmin}_{\pi \in \Pi} J_T^\pi, \quad J_T^\pi = \mathbb{E}_{\pi, T} \left[\rho_{\diamond G}(\omega) \mid s_0 \sim b_0 \right].$$

The expectation $\mathbb{E}_{\pi, T}$ is over the trajectories $\omega \in \Omega$ generated by using policy π when following the transition function T , and $\rho_{\diamond G}(\omega)$ is the cumulative cost of the trajectory ω , as in Equation (1). In the fully observable setting of MDPs, dynamic programming can compute an optimal policy and the associated expected cost for the SSP problem [6]. For POMDPs, finding optimal policies for the SSP problem is undecidable [47]. Therefore, it is common to approximate optimal policies with finite memory. A policy is *finite-memory* if it can be represented by a finite-state controller:

DEFINITION 2 (FSC). A *finite-state controller* is a tuple $\pi_f = \langle N, n_0, \delta, \eta \rangle$ where N is a finite set of memory nodes, $n_0 \in N$ the

initial node, $\delta: N \times Z \rightarrow \Delta(A)$ is the stochastic action function, and $\eta: N \times Z \rightarrow N$ is the deterministic memory update.

When $|N| = k$, the FSC is called a k -FSC, and $\Pi_f \subseteq \Pi$ denotes the (uncountable) set of all FSCs. A policy is *memoryless* when it can be represented by a 1-FSC. The expected cumulative costs (performance) $J_T^{\pi_f}$ of an FSC π_f on a POMDP M is evaluated by computing the state-values $V^{\pi_f}: S \times N \rightarrow \mathbb{R}_{\geq 0}$ on the product Markov chain [48] via dynamic programming.

Comparably to FSCs, recurrent neural networks (RNNs) are (infinite) state machines parameterized by differential functions, which we use to learn information about the history in $\mathcal{H} \subseteq \mathbb{R}^d$. The *hidden size* d defines the length of the latent history vector. Analogously to an FSC, we design the RNN to consist of a parameterized internal memory update $\hat{\eta}_\phi: \mathcal{H} \times Z \rightarrow \mathcal{H}$ that recurrently computes the new latent memory vector $\hat{h} \in \mathcal{H}$ from the observations in a history $h \in \mathcal{H}$. Thus, the RNN represents a function $\text{RNN}: \mathcal{H} \rightarrow \mathcal{H}$. When we append a fully connected layer with a softmax activation function $\sigma^\phi: \mathcal{H} \rightarrow \Delta(A)$ to the RNN, it yields an RNN policy network $\pi^\phi: \mathcal{H} \rightarrow \Delta(A)$ from histories to distributions over actions.

3 ROBUST MARKOV MODELS

A *robust* MDP (RMDP) is an MDP where the transition probabilities are not precisely given but belong to predefined sets of distributions known as the *uncertainty sets* [32, 76]. We fix a specific type of RMDP where the transition function maps to a probability interval or zero, also known as interval MDPs [20, 55].

DEFINITION 3 (RMDP). A *robust MDP with interval uncertainty* is a tuple $\mathcal{U} = \langle S, A, \mathcal{T}, C \rangle$, where S, A, C are the finite sets of states and actions and the cost function, respectively, and, $\mathcal{T}: S \times A \rightarrow (S \rightarrow \mathbb{I} \cup \{0\})$ is the uncertain transition function that maps each transition to either a probability interval in \mathbb{I} , or probability 0 whenever the transition does not exist.

The uncertainty is resolved in a game-like manner where the agent (choosing the actions) and nature (choosing probability distributions from the uncertainty sets) alternate turns [32]. For RMDPs, we assume that nature’s resolution of uncertainty is *dynamic*, i.e., nature’s choice is not restricted by any previous choice [32]. Furthermore, we assume independence between all state-action pairs, a common assumption known as (s, a) -*rectangularity* [32, 76]. Specifically, the uncertain transition function \mathcal{T} is convex and factorizes over state-action-pairs:

$$\mathcal{T} = \bigotimes_{(s,a) \in S \times A} \mathcal{T}(s, a),$$

where each $\mathcal{T}(s, a)$ is defined given the interval uncertainty model:

$$\mathcal{T}(s, a) = \left\{ T(s, a) \in \Delta(S) \mid \forall s' \in S: T(s' \mid s, a) \in \mathcal{T}(s, a)(s') \right\}.$$

Robust POMDPs [RPOMDPs; 57] extend POMDPs in a similar way that RMDPs extend MDPs by accounting for uncertainty in the transition and observation functions. Without loss of generality, we consider only uncertainty in the transition function, as any RPOMDP with an uncertain observation function can be

transformed into an equivalent RPOMDP with deterministic observations [7, Appendix B]. Just as with our definition of RMDPs, we focus on uncertainty sets given by probability intervals.

DEFINITION 4 (RPOMDP). A *robust POMDP with interval uncertainty* is a tuple $\mathcal{M} = \langle S, A, \mathcal{T}, C, Z, O \rangle$, where S, A, Z , are the sets of states, actions, and observations, and C, O are the cost and observation functions from POMDPs in Definition 1, respectively. The uncertain transition function \mathcal{T} is as defined for RMDPs (Definition 3), and we assume again (s, a) -rectangularity.

A POMDP M with transition function T is within the uncertainty set of the RPOMDP if every transition probability of T lies within its respective interval in \mathcal{T} . We may also write $T \in \mathcal{T}$ and $M \in \mathcal{M}$.

R(PO)MDPs have two optimal value functions and associated optimal policies: one where the agent and nature play *adversarially*, and one where they play *cooperatively*. The former is the robust (or pessimistic) setting, and the latter is optimistic. For ease of presentation, we focus on the robust setting for the remainder of the paper*. In R(PO)MDPs, the trajectories generated by the policy $\pi \in \Pi$ depend on the transition function $T \in \mathcal{T}$. Hence, in the robust variant of the SSP problem, our objective is to find a policy that minimizes the *worst-case expected cumulative cost* \mathcal{J}_T^π :

$$\pi^* \in \operatorname{argmin}_{\pi \in \Pi} \mathcal{J}_T^\pi, \quad \mathcal{J}_T^\pi = \sup_{T \in \mathcal{T}} J_T^\pi.$$

Robust dynamic programming. In the fully observable setting of RMDPs, optimal robust values can be computed by *robust dynamic programming* [8, 32, 55]. The optimal robust value function \underline{V}^* is the least fixed point of the following recursive equation[†]:

$$\underline{V}(s) = \min_{a \in A} \left\{ C(s, a) + \underbrace{\sup_{T(s,a) \in \mathcal{T}(s,a)} \left\{ \sum_{s' \in S} T(s' \mid s, a) \underline{V}(s') \right\}}_{\text{Inner problem}} \right\}. \quad (2)$$

Under (s, a) -rectangularity and the (dynamically resolved) interval uncertainty model, the inner optimization problem can be efficiently solved via a *bisection algorithm* [55, Section 7.2]. The optimal policy π^* , which is memoryless deterministic, is derived from the robust values \underline{V}^* by choosing the minimizing action at each state, just as in MDPs [32]. For RPOMDPs, robust dynamic programming is performed on the underlying belief model [57], just as for standard POMDPs [36], and therefore limited to small state spaces.

Objective. Given an RPOMDP $\mathcal{M} = \langle S, A, \mathcal{T}, C, Z, O \rangle$ with a set of goal states $G \subseteq S$, compute an FSC policy $\pi_f \in \Pi_f$ that minimizes the worst-case expected cumulative cost $\mathcal{J}_T^{\pi_f}$.

4 PESSIMISTIC ITERATIVE PLANNING

We present our main contributions. First, we outline the two main parts of the *pessimistic iterative planning* (PIP) framework. Subsequently, we give an overview of our algorithmic implementation of PIP, named **RFSCNET**, which computes robust finite-memory policies for RPOMDPs through optimizing an RNN.

*All our results extend to the optimistic case.

[†]To compute optimistic values \bar{V} , we substitute the supremum with an infimum.

4.1 The PIP Framework

Analogously to a two-player game, PIP iteratively executes two parts, representing the two sides of Figure 1:

- (1) Compute an FSC policy π_f for a given POMDP $M \in \mathcal{M}$.
- (2) Select a *pessimistic* POMDP $M' \in \mathcal{M}$ with respect to this FSC policy π_f , and set $M \leftarrow M'$. Give M as input to (1).

These steps are repeated in a game-like fashion. The first player executes Step (1) and computes an FSC π_f for the (non-robust) POMDP M . The aim is to *minimize* the expected cost. Note that PIP may use any existing approach that computes FSCs for (non-robust) POMDPs. The other player then executes Step (2) and determines a POMDP M' that is pessimistic with respect to π_f . Thereby, the other player effectively *maximizes* the expected cost incurred under π_f . Returning to Step (1), the first player takes M' into account and computes a new (updated) FSC that is optimized for M' .

This process is repeated until we reach a *termination criterion*, for instance, when the worst-case expected cost of the FSC satisfies a target threshold or a maximum number of iterations is reached.

Convergence. To ensure convergence of PIP in the absence of any termination criteria, both Steps (1) and (2) must satisfy certain conditions. Step (1) needs to constitute a policy improvement step. That is, akin to policy improvement theorems established for FSCs in POMDPs [22, 54, 60], the newly computed FSC needs to outperform the FSC of the previous iteration. In Step (2), the pessimistic POMDP must accurately represent the worst-case under the FSC, guaranteeing that the choice of probabilities increases the expected cost, *i.e.*, it deteriorates the policy's performance. This step bears similar characteristics to the robust policy evaluation steps of policy iteration for RMDPs [32, 38, 63, 70, 76]. Under these conditions, the PIP framework is set to converge to a local optimum, *i.e.*, an equilibrium between the improvements of the FSC policy and the selection of pessimistic POMDP instances. The feasibility of the policy improvement condition depends on the method chosen to compute the FSCs. For the feasibility of determining the worst-case probabilities, we provide more details in Section 6.

4.2 The rFSCNET Algorithm

Next, we detail the steps of our algorithm rFSCNET, which implements the two parts of PIP. Part one corresponds with Section 5 and the left-hand side in Figure 1. In this part, we compute FSCs for pessimistic POMDPs $M \in \mathcal{M}$ using an RNN, which is specific to rFSCNET. In particular, we:

- i. Compute a *supervision policy* π_M for the POMDP M (Section 5.1) and simulate π_M on M to collect the histories and the action distributions of π_M into a data set \mathcal{D} (Section 5.2).
- ii. Train the RNN policy π^θ on the data set \mathcal{D} (Section 5.3) and extract an FSC π_f (Section 5.4).

Part two corresponds to Section 6 and the right-hand side of Figure 1. Here, we implement the robust policy evaluation of a computed FSC and, subsequently, the selection of new pessimistic POMDPs. The implementation of this part applies to any implementation of PIP and is not specific to rFSCNET. In this part, we:

- iii. Evaluate the FSC π_f exactly through robust dynamic programming (Section 6.1).

- iv. Compute a new pessimistic POMDP $M' \in \mathcal{M}$ based on the FSC π_f (Section 6.2).

We determine to stop the algorithm at Step (iii.) based on the aforementioned termination criteria of the PIP framework and save the best robust policy found thus far. After Step (iv.), if we have not met a termination criterion, we start a new iteration at Step (i.).

rFSCNET can be classified as a gradient-based method to compute FSCs [2], as the RNN is trained over the iterations through stochastic gradient descent. Due to the RNN, we cannot establish a formal policy improvement guarantee for rFSCNET. However, because we extract FSCs, we establish the worst-case performance analytically. From this, we determine the POMDP that deteriorates the FSC's performance and use it to train the RNN further.

5 SUPERVISED LEARNING OF ROBUST FSCS

In this section, we specify our methods of collecting a dataset to train the RNN, the policies used to gather this data, and how to extract a finite-memory policy from an RNN. We initialize with an arbitrary POMDP instance $M \in \mathcal{M}$ as input, which adapts at each iteration to be pessimistic towards the current policy.

5.1 Supervision Policies

Recall from Section 2 that computing an optimal policy in POMDPs for our objective is undecidable. Furthermore, our iterative procedure relies on computing several policies for different POMDPs. Thus, computational efficiency is a concern, and fast approximate methods are preferred. We compute a *supervision policy* $\pi_M: \mathcal{B} \rightarrow \Delta(A)$ that approximates the optimal policy π^* for the POMDP M . In particular, we approximate the belief-based action-values $Q_M: \mathcal{B} \times A \rightarrow \mathbb{R}$ for $M \in \mathcal{M}$, which we denote by \hat{Q}_M . The supervision policy is then derived by taking a Dirac distribution on the minimizing action, such that $\pi_M(a | b) = [a = \arg\min_{a \in A} \hat{Q}_M(b, a)]$.

We use Q_{MDP} [46] and the fast-informed bound [FIB; 24] to compute the approximations Q_{MDP} and Q_{FIB} respectively. Q_{MDP} neglects information-gathering and assumes full state observability after a single step [46]. The values Q_{FIB} are tighter than those of Q_{MDP} since it factors in the observation of the next state. Although Q_{FIB} is computationally more expensive than Q_{MDP} , Q_{FIB} updates are still of polynomial complexity, allowing us to compute it for any $M \in \mathcal{M}$ efficiently, see Appendix B for more details.

While we opt for Q_{MDP} and Q_{FIB} because of their computational efficiency, other POMDP solution methods may also be used, such as *partially observable Monte Carlo planning* [65] or variants of *heuristic-search value iteration* [29, 66].

5.2 Data Generation

Before training the RNN, we generate a dataset \mathcal{D} by simulating the supervision policy π_M on the current (pessimistic) POMDP $M \in \mathcal{M}$. We execute $I \in \mathbb{N}$ simulations up to length $H \in \mathbb{N}$. During the simulations, we play the actions of the supervision policy π_M . Additionally, we aggregate the histories and associated action distributions generated by π_M .

To elaborate, at each time step $1 \leq t < H$ of simulation i , we track the beliefs $b_t^{(i)}$ associated with history $h_t^{(i)}$, using the transition function T of M , with $b_0^{(i)}$ the initial belief b_0 of the RPOMDP M .

Then, $\mu_t^{(i)} = \pi_M(\cdot | b_t^{(i)})$ is the action distributions of the supervision policy π_M during the simulation, and $a_t^{(i)} \sim \mu_t^{(i)}$ is the action used in simulation i at time t . We store the histories and action distributions in the dataset $\mathcal{D} = \{\{h_t^{(i)}, \mu_t^{(i)}\}_{t=1}^H\}_{i=1}^I$, which then consists of $I \cdot H$ histories and the associated action distributions. In the next step, we employ \mathcal{D} to train the RNN policy π^ϕ .

5.3 RNN Policy Training

The training objective for the RNN is to minimize the distance between the distributions of the RNN policy π^ϕ and the distributions μ of the supervision policy π_M over the dataset \mathcal{D} :

$$\min_{\phi} \frac{1}{|\mathcal{D}|H} \sum_{i=1}^{|\mathcal{D}|} \sum_{t=1}^H L(\pi^\phi(h_t^{(i)}) \parallel \mu_t^{(i)}), \quad (3)$$

where L is a distance or loss function, such as the Kullback-Leibler divergence, and for each batch index i and time-step t , the histories $h_t^{(i)}$ are inputs to the RNN, and the action distributions $\mu_t^{(i)}$ are the labels. We optimize the parameters ϕ of the RNN by calculating the gradient via backpropagation through time [74].

We opt for a model-based approach, using approximate solvers to compute the supervision policy π_M for $M \in \mathcal{M}$ and train the RNN to imitate π_M in a supervised manner, resembling *imitation learning* [30, 62]. Alternatively, one could employ a model-free objective such as *recurrent policy gradients* [75]. Model-free methods, however, neglect the available information from the model and, thus, require a large number of samples to converge [49, 58], and it is unclear when training should be stopped.

5.4 Extracting an FSC from an RNN

Recall that in our approach, we change the POMDP at each iteration to be pessimistic against the current policy. To find the new pessimistic POMDP $M' \in \mathcal{M}$, we need to find a finite-memory representation of the policy, which we do as follows.

We cluster the hidden memory states of the RNN [56, 77] to find a finite-memory policy in the form of an FSC. There are multiple ways to achieve such a clustering. Prior work [12] uses a quantized bottleneck network [QBN; 41] to reduce the possible memory states to a finite set. They train the QBN *post hoc* by minimizing the mean-squared error on the hidden states generated by the RNN. Alternatively, it can be trained *end-to-end* by updating its parameters with the gradient calculated from Equation (3), which we name QRNN for quantized RNN. Moreover, similar to post hoc training of the QBN, we can run a clustering algorithm such as k-means++ [4] to minimize the in-cluster variance of the hidden states. For post hoc training, we employ the histories in \mathcal{D} to generate the RNN hidden states. We consider all three methods in this paper's experiments. For more details on the QBN, we refer to Appendix D.1.

Instead of through simulations, as done by Koul et al. [41], we utilize the model to construct the FSC. The clustering determines a finite set N of memory nodes of the RNN's possible hidden states, *i.e.*, a partitioning of \mathcal{H} . We find the FSC's memory update η by executing a forward pass of the RNN's memory update $\hat{\eta}_\phi$ for each reconstruction of $n \in N$, which produces the next memory nodes $n' \in N$ and RNN hidden state $\hat{h} \in \mathcal{H}$ for each $z \in \mathcal{Z}$ by exploiting the batch dimension. Then, the action mapping δ for n and z is

given by the distribution of the RNN policy network $\sigma^\phi(\hat{h})$ for the next memory state. The RNN's initial state determines the initial node n_0 , and we prune any unreachable nodes from the FSC.

6 ROBUST POLICY EVALUATION AND PESSIMISTIC SELECTION OF POMDPs

The previous section explains how we find an FSC for (pessimistic) POMDPs. Now, we present our methods for robust policy evaluation of the FSC and, subsequently, for selecting the pessimistic, *i.e.*, worst-case POMDP $M' \in \mathcal{M}$ from the uncertainty set of the RPOMDP.

6.1 Robust Policy Evaluation

We evaluate the robust performance of the FSC on the RPOMDP via the product construction of a *robust Markov chain* (RMC), similar to the one used for evaluating FSCs in (non-robust) POMDPs [48].

DEFINITION 5 (ROBUST MARKOV CHAIN). *From an RPOMDP $\mathcal{M} = \langle S, A, \mathcal{T}, C, Z, O \rangle$ with initial belief b_0 and an FSC $\pi_f = \langle N, n_0, \eta, \delta \rangle$ we construct a robust Markov chain $\mathcal{M}^{\pi_f} = \langle S \times N, b_0^{\pi_f}, \mathcal{P}^{\pi_f}, C^{\pi_f} \rangle$ where the state-space is the product of RPOMDP states S and FSC memory nodes N , the initial state distribution is $b_0^{\pi_f}(\langle s, n \rangle) = b_0(s)[n = n_0]$. The uncertain transition and cost functions are:*

$$\begin{aligned} \mathcal{P}^{\pi_f}(\langle s, n' \rangle | \langle s, n \rangle) &= \sum_{a \in A} \mathcal{T}(s, a)(s') \delta(a | n, O(s)) [n' = \eta(n, O(s))], \\ C^{\pi_f}(\langle s, n \rangle) &= \sum_{a \in A} \delta(a | n, O(s)) C(s, a), \end{aligned}$$

where addition and multiplication over intervals follow the standard rules for interval arithmetic [27]. Let $P_T^{\pi_f} \in \mathcal{P}^{\pi_f}$ denote the (non-robust) transition function of the Markov chain by selecting the transition probabilities $T \in \mathcal{T}$ from the RPOMDP.

The *robust value* of the FSC policy π_f is determined by the robust state values of the robust Markov chain \mathcal{M}^{π_f} .

DEFINITION 6 (ROBUST POLICY EVALUATION). *The robust value function $\underline{\mathcal{V}}^{\pi_f} : S \times N \rightarrow \mathbb{R}_{\geq 0}$ is given by the robust Bellman equation:*

$$\begin{aligned} \underline{\mathcal{V}}^{\pi_f}(\langle s, n \rangle) &= C^{\pi_f}(\langle s, n \rangle) + \\ &\underbrace{\sup_{P^{\pi_f}(\langle s, n \rangle) \in \mathcal{P}^{\pi_f}(\langle s, n \rangle)} \left\{ \sum_{s' \in S} \sum_{n' \in N} P^{\pi_f}(\langle s', n' \rangle | \langle s, n \rangle) \underline{\mathcal{V}}^{\pi_f}(\langle s', n' \rangle) \right\}}_{\text{Inner problem}}. \end{aligned} \quad (4)$$

This robust value function follows directly from robust dynamic programming on \mathcal{M}^{π_f} , see Equation (2). The robust value of the policy π_f in the RPOMDP is:

$$\sum_{s \in S} \sum_{n \in N} b_0^{\pi_f}(\langle s, n \rangle) \underline{\mathcal{V}}^{\pi_f}(\langle s, n \rangle).$$

Using Definition 6, we compute the performance of any FSC extracted from the RNN and store the best FSC over the iterations based on its performance. The robust state-values $\underline{\mathcal{V}}^{\pi_f}$ also enable us to find the new associated pessimistic POMDP $M' \in \mathcal{M}$ for the next iteration of PIP.

REMARK 1 (RECTANGULARITY IN THE RMC). *The assumption of rectangularity over the product state-space of the RMC effectively leads to $(\langle s, n \rangle, a)$ -rectangularity. That is, nature's choices are independent of the agent's current memory node, yielding a value that is a*

conservative bound compared to the value where nature’s choices must be consistent with the agent’s memory node. Appendix A contains the formal statement and proof.

6.2 Selecting Pessimistic POMDP Instances

We now construct a heuristic to find a new POMDP instance $M' \in \mathcal{M}$ that constitutes the local worst-case instance for the current policy under (s, a) -rectangularity of the RPOMDP.

Let $\pi_f = \langle N, n_0, \delta, \eta \rangle$ be the current FSC. Given the robust value function \underline{V}^{π_f} computed at the previous step, we aim to find a POMDP $M' \in \mathcal{M}$ that induces its worst-case value and, thus, is pessimistic to the FSC π_f .

DEFINITION 7 (PESSIMISTIC POMDP). *Given an FSC policy π_f and its robust value function \underline{V}^{π_f} , the pessimistic POMDP $M' \in \mathcal{M}$ is the POMDP $M' = \langle S, A, \underline{T}, \underline{C}, Z, O \rangle$ with the worst-case transition function $\underline{T} \in \mathcal{T}$ with respect to the robust value function \underline{V}^{π_f} :*

$$\underline{T} \in \operatorname{argmax}_{T \in \mathcal{T}} P_T^{\pi_f} \underline{V}^{\pi_f}.$$

As mentioned in the previous subsection, the robust value function is effectively computed under $(\langle s, n \rangle, a)$ -rectangularity. Furthermore, robust dynamic programming assumes that nature can choose different probabilities, *i.e.*, dynamically, at each iteration. When we extract an pessimistic POMDP, we desire a POMDP where nature chooses a single probability, *i.e.*, *static* uncertainty [7, 32], for each interval. Therefore, we compute the following transition probabilities for all $(s, a) \in S \times A$ under the additional constraints that (1) probabilities are dependent on the memory nodes $n \in N$, *i.e.*, under (s, a) -rectangularity, and (2) that there is a single fixed probability each time a state-action pair is encountered:

$$\operatorname{argmax}_{T(s,a) \in \mathcal{T}(s,a)} \sum_{n \in N} \sum_{s' \in S} \sum_{n' \in N} P_T^{\pi_f}(\langle s', n' \rangle | \langle s, n \rangle) \underline{V}^{\pi_f}(\langle s', n' \rangle).$$

Informally, it can be understood as solving the inner problem of Equation (4) once more under these additional constraints.

We construct a linear program (LP) that precisely encodes our requirements. Let $\hat{T}_{s,a,s'}$ be the optimization variables representing the transition function probabilities. The LP is then given by:

$$\begin{aligned} \max_{\hat{T}} \quad & \sum_{s,n,a,s',n'} \hat{T}_{s,a,s'} \delta(a | n, O(s)) [n' = \eta(n, O(s))] \underline{V}^{\pi_f}(\langle s', n' \rangle) \\ \text{s.t. } \quad & \forall s, a \in S \times A: \sum_{s' \in S} \hat{T}_{s,a,s'} = 1, \\ & \forall s, a, s' \in S \times A \times S: \hat{T}_{s,a,s'} \in \mathcal{T}(s, a)(s'). \end{aligned} \quad (5)$$

Solving this LP yields assignments for the variables $\hat{T}_{s,a,s'}$ that determine the *worst-case transition function* $\hat{T}: S \times A \rightarrow \Delta(S)$ that satisfies $\hat{T}(s, a) \in \mathcal{T}(s, a)$ for all $(s, a) \in S \times A$.

By construction, the assignments are valid probability distributions within each respective interval and yield a heuristic for the worst possible value for the given FSC under (s, a) -rectangularity. The variables $\hat{T}_{s,a,s'}$ constitute the probabilities of the transition function \hat{T} for the *pessimistic* POMDP $M' = \langle S, A, \hat{T}, \underline{C}, Z, O \rangle$.

With the computation of M' , we have closed the loop of PIP. With this pessimistic POMDP instance $M' \in \mathcal{M}$, we resume execution from the first step in Section 5 of our implementation of PIP until we reach a termination criterion.

7 EXPERIMENTAL EVALUATION

We empirically assess different aspects of rFSCNET to address the following questions:

- (Q1) **Robustness and baseline comparison.** How does rFSCNET compare to various baselines that do not utilize the PIP framework: does PIP enable robust performance?
- (Q2) **Comparison with the state-of-the-art.** How does rFSCNET’s performance compare to SCP [17], a state-of-the-art method to compute finite-memory policies for RPOMDPs?
- (Q3) **Memory size sensitivity.** How does the FSC size affect rFSCNET and SCP’s performance?
- (Q4) **Configuration sensitivity.** How do different configurations of supervision policies and clustering methods affect the performance of rFSCNET?

Environments. We extend four POMDP environments to RPOMDPs: an *Aircraft* collision avoidance problem [17, 40], and three grid-worlds with adversaries named *Avoid*, *Evade*, and *Intercept* [34]. On *Aircraft*, the agent is tasked to avoid a collision with an intruder aircraft while accounting for uncertainty in the probabilities of the pilot’s responsiveness and the intruder changing direction, both mapping to a $[0.6, 0.8]$ interval. The grid-world environments model the probability of taking multiple steps instead of a single one for each possible moving action, given by the interval $[0.1, 0.4]$. We provide environment descriptions and dimensions, run times, and details on the tools and hyperparameters used in Appendices C, E and G, respectively.

Baselines. We consider baselines to evaluate the impact of the pessimistic selection of POMDPs of the PIP framework on robust performance. The baselines train either on a fixed POMDP throughout the iteration, (1) initialized randomly or (2) by the lower or upper bound of the uncertainty set, or (3) on random POMDPs at each iteration, resembling the practice of *domain randomization* [72].

Metrics. We compare the performance, *i.e.*, *robust values*, of the computed FSCs. For rFSCNET and the baselines, we consider the best robust value found across the iterations. As these methods exhibit randomness due to sampling and initialization, we report statistics of the robust value across 20 seeds. SCP is not dependent on randomness, and we only report a single value.

7.1 Analysis

Figure 2 compares the performance of rFSCNET to the aforementioned baselines. Table 1 shows rFSCNET’s median and minimum performance when configured with a maximal memory size of $k = 9$, compared to the SCP method with two different sizes $k \in \{3, 9\}$. Additionally, the heatmaps in Figure 3 showcase the effect of various memory sizes k on the performance of both rFSCNET and SCP in *Aircraft* and *Evade*. In these results, rFSCNET is equipped with k-means++ clustering and QMDP as supervision policy. Figure 4 shows the difference in training performance, in terms of the RNN and QBN losses, between rFSCNET and a baseline on *Intercept*. Figure 5 compares rFSCNET across multiple supervision policy and clustering configurations to a baseline on *Intercept*. Appendix F provides the complete set of results. We now address each research question based on these results.

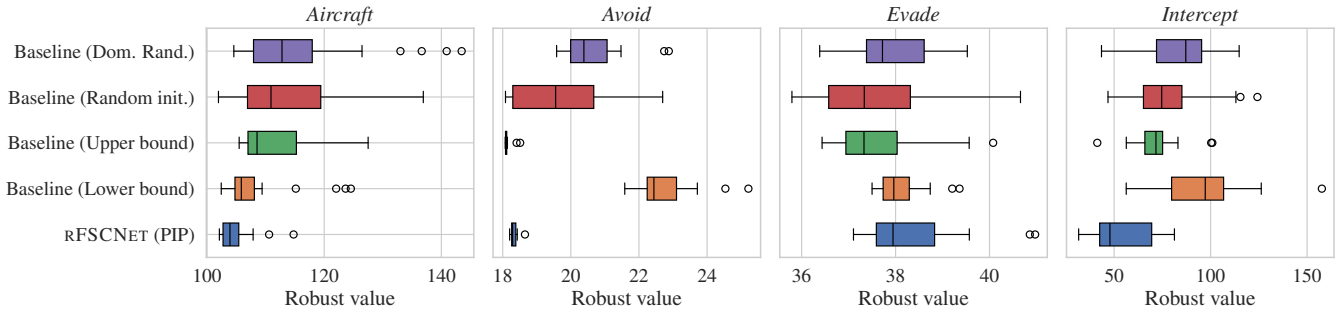


Figure 2: Boxplots depicting the minimum (i.e., best) robust value of the extracted FSC policies for both rFSCNET and the baselines across 20 seeds, all configured with QMDP and k-means++.

		<i>Aircraft</i>	<i>Avoid</i>	<i>Evade</i>	<i>Intercept</i>
RMDP (LB)	\mathcal{V}^*	94.24	18.05	31.19	16.99
SCP	$k = 3$	116.03	20.07	37.97	31.57
	$k = 9$	116.58	29.51	39.78	101.12
rFSCNET	med.	103.30	18.51	37.61	56.20
	min.	102.03	18.16	36.65	34.95

Table 1: The median (med.) and minimum (min.) of the best values (lower is better) that were found across 20 seeds by rFSCNET compared to the values of SCP. The lower bound (LB) is the optimal robust value \mathcal{V}^* of the underlying RMDP, ignoring partial observability. We highlight the best value between SCP’s values and the median value of rFSCNET.

(Q1) Comparison to baselines. As seen in Figure 2, on *Aircraft* and *Intercept*, rFSCNET outperforms all baselines, reaching a median value across the seeds lower than the first quartile of all baselines. On average, rFSCNET incurs lower expected costs than the baselines. Figure 4 shows that in the *Intercept* environment, training on pessimistic POMDPs, instead of a single fixed POMDP, is a more difficult learning target. Even though this makes the training task more challenging, rFSCNET still performs well. The results are more ambiguous in the *Evade* environment. The baselines can perform better, demonstrating that ignoring the model uncertainty may suffice in this environment. Nonetheless, we still observe that rFSCNET achieves at least the same robust performance as the baselines. On *Avoid*, rFSCNET performs slightly worse than the baseline that is trained on the upper bound of the uncertainty set, while the remaining baselines clearly perform very poorly. We conjecture that, by coincidence, the upper bounds provide an adequate approximation of the worst-case probabilities. rFSCNET, without this particular initialization, still achieves comparable performance to this baseline. Good performance of the baselines is not guaranteed, and the baselines may find much worse performing policies, as evidenced by the results obtained when trained on the lower bound or through domain randomization. We conclude that the baselines are unreliable as they are sensitive to the POMDPs used throughout training, while rFSCNET performs reliably across environments.

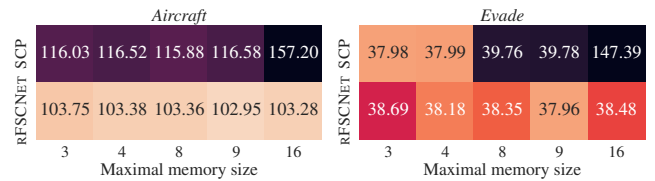


Figure 3: Heatmaps comparing the median robust value of rFSCNET to SCP’s robust value under various memory sizes.

(Q2) Comparison with the state-of-the-art. As seen in Table 1, in comparison to rFSCNET, SCP performs comparably on *Evade* and best on *Intercept* when $k = 3$. rFSCNET outperforms SCP on *Aircraft*, *Avoid*, and *Evade* by both the median and minimum performance across the 20 seeds. When the memory size in SCP is set to $k = 9$, the same maximal memory size we set for rFSCNET in these results, rFSCNET outperforms SCP across all benchmarks, both in median and minimum performance. Therefore, we can conclude that rFSCNET improves over the state-of-the-art.

(Q3) Memory size sensitivity. Table 1 indicates that SCP performs worse with more memory, especially on *Avoid* and *Intercept*. To investigate further, we conduct additional experiments to compare the performance of SCP and rFSCNET on *Aircraft* and *Evade* with increasing memory sizes. The heatmaps of Figure 3 show that SCP also performs much worse on *Aircraft* and *Evade* when more memory is specified, as indicated by the high values. A higher memory size implies more optimization variables for SCP, which may be a reason for the worse results, as SCP may get stuck in worse local optima when we allow for more memory. In contrast, rFSCNET is not sensitive to specifying more memory nodes than necessary, exhibiting consistent performance across the memory sizes. These results demonstrate the benefit of learning the memory structure instead of specifying it beforehand, as done in SCP.

(Q4) Configuration sensitivity. Figure 5 depicts the performance of rFSCNET across various configurations on *Intercept*. Figure 6 in Appendix F.1 shows these results also for the other three environments. From our results, we did not observe a major difference between using QMDP and QFIB as supervision policies. While sometimes producing better results, training the QBN *end-to-end* proves

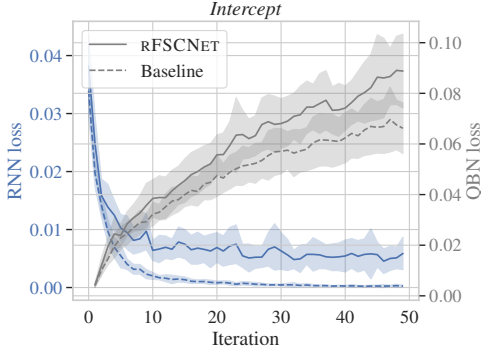


Figure 4: The *post hoc* QBN and RNN training losses from the run with Q_{MDP} averaged over iterations on *Intercept*.

less stable than *post hoc*. Overall, clustering with k-means++ produces the best results in our benchmarks. The results demonstrate that, while the configuration does impact performance, RFSCNET performs consistently across configurations.

7.2 Discussion

The results show that RFSCNET finds better robust policies than both SCP and the baseline methods, positively answering research questions (1) and (2). To RFSCNET’s merit, our results also show that a learning-based approach through the RNN has the advantage of flexibility in determining the memory structure and sizes of the FSCs, positively answering research question (3). While RFSCNET allows for various configurations, it performs consistently, positively answering question (4).

The performance of the FSCs is also impacted by the quality of discretization of the hidden states of the RNN, and faulty extraction of the FSC from the RNN leads to finding a worst-case that is not informative. How to optimally extract finite-state representations of RNNs is still an open problem. In this paper, we tested multiple options based on clustering. We emphasize that the PIP framework is modular and allows other methods that compute FSCs for POMDPs to be used instead.

Finally, we note that the performance of RFSCNET is limited by the quality of the supervision policies we compute during training. This limitation could, for instance, explain why RFSCNET performs worst on *Intercept*, as this benchmark relies on information gathering, an aspect on which Q_{MDP} is known to perform poorly. Nonetheless, RFSCNET’s modularity allows for any POMDP policy to be applied as a supervision policy in the RNN’s training procedure, allowing for trade-offs between quality and computational efficiency, depending on the task.

8 RELATED WORK

Computing optimal robust policies for RMDPs has been studied extensively [32, 38, 55, 70, 76]. RMDPs are also used in model-based (robust) reinforcement learning (RL) to explicitly account for model uncertainty and enable efficient exploration [33, 50, 59, 69].

For RPOMDPs, early works extend value iteration and point-based methods to account for the additional uncertainty [31, 57], or

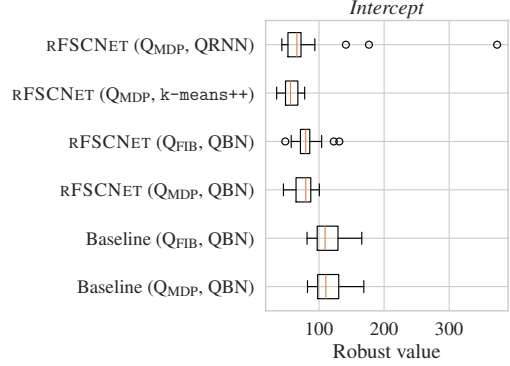


Figure 5: Boxplots of the best robust values across seeds on multiple configurations tested for RFSCNET and a baseline.

use sampling over the uncertainty sets [9]. Nakao et al. [51] extend value iteration for *distributionally robust* POMDPs, where the agent receives side information after a decision period, which is a less conservative setting. Extensions to value iteration for RPOMDPs typically do not scale well to the large state spaces (up to 13000+) we consider in this paper. Ni and Liu [53, 54] introduce a policy iteration algorithm for optimistic policies. Chamie and Mostafa [14] consider robustifying a given POMDP policy to combat sensor imprecision. Recent methods compute FSCs for RPOMDPs via quadratic [68] or sequential [17] convex programming. In contrast to our work, the convex optimization methods compute FSCs of a predefined size and structure and cannot compute FSCs in the optimistic case.

In RL, policy gradient algorithms incorporate memory using RNNs [75]. After that, RNNs serve as the baseline neural architecture for RL in POMDPs [52]. Recently, Wang et al. [73] trained a stochastic recurrent memory representation for (non-robust) POMDPs. RNNs have also successfully been used in a planning setting to compute FSCs for (non-robust) POMDPs [11–13].

9 CONCLUSION

We presented PIP, a novel planning framework for robust POMDPs. Our framework implementation, RFSCNET, utilizes RNNs to compute FSCs for the pessimistic POMDPs selected by PIP, allowing the memory structure to be learned from data. Our experiments show that our approach yields more robust policies than the baseline approaches. Additionally, RFSCNET is less sensitive to overparameterization of memory size than SCP, and outperforms the state-of-the-art SCP solver in three out of four benchmarks considered in this paper. Future work may investigate alleviating the limitation of the supervision policies by optimizing the RNN with a more sophisticated training objective or by considering more advanced supervision policies.

ACKNOWLEDGMENTS

We thank the anonymous reviewers for their valuable feedback, Eline M. Bovy and Merlijn Krale for their helpful discussions on this work, and Niels Neerhoff for allowing us to use the code of his master’s thesis. This research has been partially funded by the

NWO grant NWA.1160.18.238 (PrimaVera) and the ERC Starting Grant 101077178 (DEUCE).

REFERENCES

- [1] Martín Abadi, Paul Barham, Jianmin Chen, Zhifeng Chen, et al. 2016. Tensorflow: A system for large-scale machine learning. In *OSDI*, Vol. 16. 265–283.
- [2] Doug Aberdeen. 2003. *Policy-gradient algorithms for partially observable Markov decision processes*. Ph.D. Dissertation. The Australian National University.
- [3] Douglas Aberdeen and Jonathan Baxter. 2002. Scalable Internal-State Policy-Gradient Methods for POMDPs. In *ICML*. Morgan Kaufmann, 3–10.
- [4] David Arthur and Sergei Vassilvitskii. 2007. k-means++: the advantages of careful seeding. In *SODA*. SIAM, 1027–1035.
- [5] Bram Bakker. 2001. Reinforcement Learning with Long Short-Term Memory. In *Advances in Neural Information Processing Systems (NIPS)*. MIT Press, 1475–1482.
- [6] Dimitri P. Bertsekas. 2005. *Dynamic programming and optimal control, 3rd Edition*. Athena Scientific.
- [7] Eline M. Bovy, Marnix Suilen, Sebastian Junges, and Nils Jansen. 2024. Imprecise Probabilities Meet Partial Observability: Game Semantics for Robust POMDPs. In *IJCAI*. ijcai.org, 6697–6706.
- [8] Olivier Buffet and Douglas Aberdeen. 2005. Robust Planning with (L)RTDP. In *IJCAI*. Professional Book Center, 1214–1219.
- [9] Brendan Burns and Oliver Brock. 2007. Sampling-Based Motion Planning With Sensing Uncertainty. In *ICRA*. IEEE, 3313–3318.
- [10] Steven Carr, Nils Jansen, Sebastian Junges, and Ufuk Topcu. 2023. Safe Reinforcement Learning via Shielding under Partial Observability. In *AAAI*. AAAI Press, 14748–14756.
- [11] Steven Carr, Nils Jansen, and Ufuk Topcu. 2020. Verifiable RNN-Based Policies for POMDPs Under Temporal Logic Constraints. In *International Joint Conference on Artificial Intelligence (IJCAI)*. IJCAI.org, 4121–4127.
- [12] Steven Carr, Nils Jansen, and Ufuk Topcu. 2021. Task-Aware Verifiable RNN-Based Policies for Partially Observable Markov Decision Processes. *J. Artif. Intell. Res.* 72 (2021), 819–847.
- [13] Steven Carr, Nils Jansen, Ralf Wimmer, Alexandru Constantin Serban, Bernd Becker, and Ufuk Topcu. 2019. Counterexample-Guided Strategy Improvement for POMDPs Using Recurrent Neural Networks. In *IJCAI*. ijcai.org, 5532–5539.
- [14] Mahmoud El Chamie and Hala Mostafa. 2018. Robust Action Selection in Partially Observable Markov Decision Processes with Model Uncertainty. In *CDC*. IEEE, 5586–5591.
- [15] Krishnendu Chatterjee, Martin Chmelik, Raghav Gupta, and Ayush Kanodia. 2015. Qualitative analysis of POMDPs with temporal logic specifications for robotics applications. In *ICRA*. IEEE, 325–330.
- [16] Kyunghyun Cho, Bart van Merriënboer, Çağlar Gülçehre, Dzmitry Bahdanau, Fethi Bougares, Holger Schwenk, and Yoshua Bengio. 2014. Learning Phrase Representations using RNN Encoder-Decoder for Statistical Machine Translation. In *EMNLP*. ACL, 1724–1734.
- [17] Murat Cubuktepe, Nils Jansen, Sebastian Junges, Ahmadreza Marandi, Marnix Suilen, and Ufuk Topcu. 2021. Robust Finite-State Controllers for Uncertain POMDPs. In *AAAI*. AAAI Press, 11792–11800.
- [18] Vojtech Forejt, Marta Z. Kwiatkowska, Gethin Norman, and David Parker. 2011. Automated Verification Techniques for Probabilistic Systems. In *SFM (Lecture Notes in Computer Science, Vol. 6659)*. Springer, 53–113.
- [19] Lukas Geiger and Plummerai Team. 2020. Larq: An Open-Source Library for Training Binarized Neural Networks. *Journal of Open Source Software* 5, 45 (2020), 1746. <https://doi.org/10.21105/joss.01746>
- [20] Robert Givan, Sonia M. Leach, and Thomas L. Dean. 2000. Bounded-parameter Markov decision processes. *Artif. Intell.* 122, 1-2 (2000), 71–109.
- [21] Gurobi Optimization, LLC. 2023. Gurobi Optimizer Reference Manual. <https://www.gurobi.com>
- [22] Eric A. Hansen. 1997. An Improved Policy Iteration Algorithm for Partially Observable MDPs. In *NIPS*. The MIT Press, 1015–1021.
- [23] Matthew J. Hausknecht and Peter Stone. 2015. Deep Recurrent Q-Learning for Partially Observable MDPs. In *Proceedings of the AAAI Conference on Artificial Intelligence (AAAI)*. AAAI Press, 29–37.
- [24] Milos Hauskrecht. 2000. Value-function approximations for partially observable Markov decision processes. *Journal of Artificial Intelligence Research (JAIR)* 13 (2000), 33–94.
- [25] Nicolas Heess, Gregory Wayne, David Silver, Timothy P. Lillicrap, Tom Erez, and Yuval Tassa. 2015. Learning Continuous Control Policies by Stochastic Value Gradients. In *NIPS*. 2944–2952.
- [26] Christian Hensel, Sebastian Junges, Joost-Pieter Katoen, Tim Quatmann, and Matthias Volk. 2022. The probabilistic model checker Storm. *Int. J. Softw. Tools Technol. Transf.* 24, 4 (2022), 589–610.
- [27] Timothy J. Hickey, Qun Ju, and Maarten H. van Emden. 2001. Interval arithmetic: From principles to implementation. *J. ACM* 48, 5 (2001), 1038–1068.
- [28] Sepp Hochreiter and Jürgen Schmidhuber. 1997. Long Short-Term Memory. *Neural Comput.* 9, 8 (1997), 1735–1780.
- [29] Karel Horák, Branislav Bosanský, and Krishnendu Chatterjee. 2018. Goal-HSVI: Heuristic Search Value Iteration for Goal POMDPs. In *IJCAI*. ijcai.org, 4764–4770.
- [30] Ahmed Hussein, Mohamed Medhat Gaber, Eyad Elyan, and Christina Jayne. 2017. Imitation Learning: A Survey of Learning Methods. *ACM Comput. Surv.* 50, 2 (2017), 21:1–21:35.
- [31] Hideaki Itoh and Kiyohiko Nakamura. 2007. Partially observable Markov decision processes with imprecise parameters. *Artif. Intell.* 171, 8-9 (2007), 453–490.
- [32] Garud N. Iyengar. 2005. Robust Dynamic Programming. *Math. Oper. Res.* 30, 2 (2005), 257–280.
- [33] Thomas Jaksch, Ronald Ortner, and Peter Auer. 2010. Near-optimal Regret Bounds for Reinforcement Learning. *J. Mach. Learn. Res.* 11 (2010), 1563–1600.
- [34] Sebastian Junges, Nils Jansen, and Sanjit A. Seshia. 2021. Enforcing Almost-Sure Reachability in POMDPs. In *Computer Aided Verification (CAV) (Lecture Notes in Computer Science, Vol. 12760)*. Springer, 602–625.
- [35] Sebastian Junges, Nils Jansen, Ralf Wimmer, Tim Quatmann, Leonore Winterer, Joost-Pieter Katoen, and Bernd Becker. 2018. Finite-State Controllers of POMDPs using Parameter Synthesis. In *Conference on Uncertainty in Artificial Intelligence (UAI)*. AUAI Press, 519–529.
- [36] Leslie Pack Kaelbling, Michael L. Littman, and Anthony R. Cassandra. 1998. Planning and acting in partially observable stochastic domains. *Artificial Intelligence* 101, 1 (1998), 99–134.
- [37] Suresh Kalyanasundaram, Edwin K. P. Chong, and Ness B. Shroff. 2002. Markov decision processes with uncertain transition rates: sensitivity and robust control. In *CDC*. IEEE, 3799–3804.
- [38] David L. Kaufman and Andrew J. Schaefer. 2013. Robust Modified Policy Iteration. *INFORMS J. Comput.* 25, 3 (2013), 396–410.
- [39] Diederik P. Kingma and Jimmy Ba. 2015. Adam: A Method for Stochastic Optimization. In *International Conference on Learning Representations (ICLR)*.
- [40] Mykel J. Kochenderfer, Christopher Amato, Girish Chowdhary, Jonathan P. How, Hayley J. Davison Reynolds, Jason R. Thornton, Pedro A. Torres-Carrasquillo, N. Kemal Ure, and John Vian. 2015. *Optimized Airborne Collision Avoidance*. 249–276.
- [41] Anurag Koul, Alan Fern, and Sam Greystan. 2019. Learning Finite State Representations of Recurrent Policy Networks. In *ICLR (Poster)*. OpenReview.net.
- [42] Hanna Kurniawati, David Hsu, and Wee Sun Lee. 2008. SARSOP: Efficient Point-Based POMDP Planning by Approximating Optimally Reachable Belief Spaces. In *Robotics: Science and Systems (RSS)*. MIT Press.
- [43] Marta Kwiatkowska, Gethin Norman, and David Parker. 2011. PRISM 4.0: Verification of Probabilistic Real-Time Systems. In *Computer Aided Verification (CAV) (Lecture Notes in Computer Science, Vol. 6806)*. Springer, 585–591.
- [44] Gaspard Lambrechts, Adrien Bolland, and Damien Ernst. 2022. Recurrent networks, hidden states and beliefs in partially observable environments. *Trans. Mach. Learn. Res.* 2022 (2022).
- [45] Fengfu Li and Bin Liu. 2016. Ternary Weight Networks. *CoRR* abs/1605.04711 (2016). <http://arxiv.org/abs/1605.04711>
- [46] Michael L. Littman, Anthony R. Cassandra, and Leslie Pack Kaelbling. 1995. Learning Policies for Partially Observable Environments: Scaling Up. In *Proceedings of the Twelfth International Conference on Machine Learning*. Morgan Kaufmann, 362–370.
- [47] Omid Madani, Steve Hanks, and Anne Condon. 2003. On the undecidability of probabilistic planning and related stochastic optimization problems. *Artif. Intell.* 147, 1-2 (2003), 5–34.
- [48] Nicolas Meuleau, Kee-Eung Kim, Leslie Pack Kaelbling, and Anthony R. Cassandra. 1999. Solving POMDPs by Searching the Space of Finite Policies. In *UAI*. Morgan Kaufmann, 417–426.
- [49] Thomas M. Moerland, Joost Broekens, and Catholijn M. Jonker. 2020. Model-based Reinforcement Learning: A Survey. *CoRR* abs/2006.16712 (2020).
- [50] Janosch Moos, Kay Hansel, Hany Abdulsamad, Svenja Stark, Debora Clever, and Jan Peters. 2022. Robust Reinforcement Learning: A Review of Foundations and Recent Advances. *Mach. Learn. Knowl. Extr.* 4, 1 (2022), 276–315.
- [51] Hideaki Nakao, Ruiwei Jiang, and Siqian Shen. 2021. Distributionally Robust Partially Observable Markov Decision Process with Moment-Based Ambiguity. *SIAM J. Optim.* 31, 1 (2021), 461–488.
- [52] Tianwei Ni, Benjamin Eysenbach, and Ruslan Salakhutdinov. 2022. Recurrent Model-Free RL Can Be a Strong Baseline for Many POMDPs. In *ICML (Proceedings of Machine Learning Research, Vol. 162)*. PMLR, 16691–16723.
- [53] Yaodong Ni and Zhi-Qiang Liu. 2008. Bounded-Parameter Partially Observable Markov Decision Processes. In *ICAPS*. AAAI, 240–247.
- [54] Yaodong Ni and Zhi-Qiang Liu. 2013. Policy iteration for bounded-parameter POMDPs. *Soft Comput.* 17, 4 (2013), 537–548.
- [55] Arnab Nilim and Laurent El Ghaoui. 2005. Robust Control of Markov Decision Processes with Uncertain Transition Matrices. *Oper. Res.* 53, 5 (2005), 780–798.
- [56] Christian W. Omlin and C. Lee Giles. 1996. Extraction of rules from discrete-time recurrent neural networks. *Neural Networks* 9, 1 (1996), 41–52.
- [57] Takayuki Osogami. 2015. Robust partially observable Markov decision process. In *ICML (JMLR Workshop and Conference Proceedings, Vol. 37)*. JMLR.org, 106–115.
- [58] Jan Peters and Stefan Schaal. 2006. Policy Gradient Methods for Robotics. In *IROS*. IEEE, 2219–2225.

- [59] Marek Petrik and Dharmashankar Subramanian. 2014. RAAM: The Benefits of Robustness in Approximating Aggregated MDPs in Reinforcement Learning. In *NIPS*. 1979–1987.
- [60] Pascal Poupart and Craig Boutilier. 2003. Bounded Finite State Controllers. In *Advances in Neural Information Processing Systems (NIPS)*. MIT Press, 823–830.
- [61] Martin L. Puterman. 1994. *Markov Decision Processes: Discrete Stochastic Dynamic Programming*. Wiley.
- [62] Stéphane Ross, Geoffrey J. Gordon, and Drew Bagnell. 2011. A Reduction of Imitation Learning and Structured Prediction to No-Regret Online Learning. In *AISTATS (JMLR Proceedings, Vol. 15)*. JMLR.org, 627–635.
- [63] Jay K. Satia and Roy E. Lave Jr. 1973. Markovian Decision Processes with Uncertain Transition Probabilities. *Oper. Res.* 21, 3 (1973), 728–740.
- [64] Andrew M. Saxe, James L. McClelland, and Surya Ganguli. 2014. Exact solutions to the nonlinear dynamics of learning in deep linear neural networks. In *ICLR*.
- [65] David Silver and Joel Veness. 2010. Monte-Carlo planning in large POMDPs. In *Advances in Neural Information Processing Systems (NIPS)*. MIT Press, 2164–2172.
- [66] Trey Smith and Reid Simmons. 2004. Heuristic search value iteration for POMDPs. In *Conference on Uncertainty in Artificial Intelligence (UAI)*. AUAI Press, 520–527.
- [67] Matthijs T J Spaan. 2012. Partially Observable Markov Decision Processes. In *Reinforcement Learning: State-of-the-Art*, Marco Wiering and Martijn van Otterlo (Eds.). Springer Berlin Heidelberg, Berlin, Heidelberg, 387–414.
- [68] Marnix Suilen, Nils Jansen, Murat Cubuktepe, and Ufuk Topcu. 2020. Robust Policy Synthesis for Uncertain POMDPs via Convex Optimization. In *IJCAI*. ijcai.org, 4113–4120.
- [69] Marnix Suilen, Thiago D. Simão, David Parker, and Nils Jansen. 2022. Robust Anytime Learning of Markov Decision Processes. In *NeurIPS*.
- [70] Aviv Tamar, Shie Mannor, and Huan Xu. 2014. Scaling Up Robust MDPs using Function Approximation. In *ICML (JMLR Workshop and Conference Proceedings, Vol. 32)*. JMLR.org, 181–189.
- [71] Sebastian Thrun, Wolfram Burgard, and Dieter Fox. 2005. *Probabilistic robotics*. MIT Press.
- [72] Josh Tobin, Rachel Fong, Alex Ray, Jonas Schneider, Wojciech Zaremba, and Pieter Abbeel. 2017. Domain randomization for transferring deep neural networks from simulation to the real world. In *IROS*. IEEE, 23–30.
- [73] Andrew Wang, Andrew C. Li, Toryn Q. Klassen, Rodrigo Toro Icarte, and Sheila A. McIlraith. 2023. Learning Belief Representations for Partially Observable Deep RL. In *ICML (Proceedings of Machine Learning Research, Vol. 202)*. PMLR, 35970–35988.
- [74] Paul J. Werbos. 1990. Backpropagation through time: what it does and how to do it. *Proc. IEEE* 78, 10 (1990), 1550–1560.
- [75] Daan Wierstra, Alexander Förster, Jan Peters, and Jürgen Schmidhuber. 2007. Solving Deep Memory POMDPs with Recurrent Policy Gradients. In *ICANN (1) (Lecture Notes in Computer Science, Vol. 4668)*. Springer, 697–706.
- [76] Wolfram Wiesemann, Daniel Kuhn, and Berç Rustem. 2013. Robust Markov Decision Processes. *Math. Oper. Res.* 38, 1 (2013), 153–183.
- [77] Zheng Zeng, Rodney M. Goodman, and Padhraic Smyth. 1993. Learning Finite State Machines With Self-Clustering Recurrent Networks. *Neural Comput.* 5, 6 (1993), 976–990.

APPENDIX

A ROBUST POLICY EVALUATION

In this appendix, we show that robust policy evaluation (Definition 6) indeed provides a conservative upper bound, as described in Remark 1.

DEFINITION 8 (ROBUST MARKOV CHAIN AND ROBUST POLICY EVALUATION (EXTENDED)). *Given an RPOMDP $\mathcal{M} = \langle S, A, \mathcal{T}, C, Z, O \rangle$ with initial state distribution (belief) b_0 and an FSC $\pi_f = \langle N, n_0, \eta, \delta \rangle$, the robust state-values of \mathcal{M} under F , $\underline{V}^{\pi_f} : S \times N \rightarrow \mathbb{R}$, are given by the state-values in the robust Markov chain $\langle S \times N, \mathcal{P}^{\pi_f}, C^{\pi_f} \rangle$ where the states are the product of RPOMDP states S and FSC memory nodes N , and the uncertain transition and cost functions are:*

$$\begin{aligned}\mathcal{P}^{\pi_f}(\langle s', n' \rangle \mid \langle s, n \rangle, a) &= \mathcal{T}(s' \mid s, a) \delta(a \mid n, O(s)) [n' = \eta(n, O(s))] \\ \mathcal{P}^{\pi_f}(\langle s', n' \rangle \mid \langle s, n \rangle) &= \sum_{a \in A} \mathcal{P}^{\pi_f}(\langle s', n' \rangle \mid \langle s, n \rangle, a) \\ C^{\pi_f}(\langle s, n \rangle) &= \sum_{a \in A} \delta(a \mid n, O(s)) C(s, a),\end{aligned}$$

where addition and multiplication over intervals follow the standard rules for interval arithmetic [27]. For completeness, the uncertainty sets of the uncertain transition function of the RMC are defined as:

$$\mathcal{P}^{\pi_f}(\langle s, n \rangle, a) = \left\{ T(s, a) \delta(a \mid n, O(s)) \in \Delta(S \times N) \mid \forall \langle s', n' \rangle \in S \times N: T(s' \mid s, a) \in \mathcal{T}(s, a)(s') \wedge [n' = \eta(n, O(s))] \right\}. \quad (6)$$

$$\mathcal{P}^{\pi_f}(\langle s, n \rangle) = \left\{ \sum_{a \in A} T(s, a) \delta(a \mid n, O(s)) \in \Delta(S \times N) \mid \forall \langle s', n' \rangle \in S \times N: T(s' \mid s, a) \in \mathcal{T}(s, a)(s') \wedge [n' = \eta(n, O(s))] \right\}. \quad (7)$$

Then, the robust state-values are defined as:

$$\underline{V}^{\pi_f}(\langle s, n \rangle) = C^{\pi_f}(\langle s, n \rangle) + \sup_{P^{\pi_f}(\langle s, n \rangle) \in \mathcal{P}^{\pi_f}(\langle s, n \rangle)} \sum_{s' \in S} \sum_{n' \in N} P^{\pi_f}(\langle s', n' \rangle \mid \langle s, n \rangle) \underline{V}^{\pi_f}(\langle s', n' \rangle). \quad (8)$$

Under strict (s, a) -rectangularity of the RPOMDP, we would have the following robust Bellman equation to solve:

$$\underline{V}_{\star}^{\pi_f}(\langle s, n \rangle) = \left(C^{\pi_f}(\langle s, n \rangle) + \sum_{a \in A} \sup_{T(s, a) \in \mathcal{T}(s, a)} \left\{ \sum_{s' \in S} \sum_{n' \in N} P_T^{\pi_f}(\langle s', n' \rangle \mid \langle s, n \rangle, a) \underline{V}_{\star}^{\pi_f}(\langle s', n' \rangle) \right\} \right).$$

The inner optimization problem is convex under (s, a) -rectangular and interval uncertainty sets, but solving it at each dynamic programming step requires $|S||A|$ linear programs. Furthermore, it is unclear how to constrain the inner supremum so that the same probabilities are picked at each memory node $n \in N$ of the FSC. However, for computational tractability, we instead opt to assume full (s, a) -rectangularity on the product state-space of the RMC, effectively leading to $\langle s, n \rangle, a$ -rectangularity. Below, we establish that this provides a conservative upper bound.

For an initial belief b_0 and initial memory node n_0 , both state-based value functions can be extended to the value in the initial belief:

$$\begin{aligned}\underline{V}_{\star}^{\pi_f}(\langle b_0, n_0 \rangle) &= \sum_{s \in S} b_0(s) \underline{V}_{\star}^{\pi_f}(\langle s, n_0 \rangle), \\ \underline{V}^{\pi_f}(\langle b_0, n_0 \rangle) &= \sum_{s \in S} b_0(s) \underline{V}^{\pi_f}(\langle s, n_0 \rangle).\end{aligned}$$

THEOREM 1. *Given the FSC π_f , the robust state-values \underline{V}^{π_f} of the robust Markov chain $\langle S \times N, b_0^{\pi_f}, T^{\pi_f}, C^{\pi_f} \rangle$ provide a (conservative) upper bound on the value $\underline{V}_{\star}^{\pi_f}$ of F under (s, a) -rectangularity in the RPOMDP with initial belief b_0 . That is, $\underline{V}_{\star}^{\pi_f}(\langle s, n \rangle) \leq \underline{V}^{\pi_f}(\langle s, n \rangle)$, and consequently $\underline{V}_{\star}^{\pi_f}(\langle b_0, n_0 \rangle) \leq \underline{V}^{\pi_f}(\langle b_0, n_0 \rangle)$.*

PROOF. We show that $\underline{V}^{\pi_f}(\langle s, n \rangle) \geq \underline{V}_{\star}^{\pi_f}(\langle s, n \rangle)$ for all $(\langle s, n \rangle) \in S \times N$. Recall Equation (8). Omitting the constant $C^{\pi_f}(\langle s, n \rangle)$, we rewrite the inner supremum of the equation as follows:

$$\begin{aligned}\underline{V}^{\pi_f}(\langle s, n \rangle) &= C^{\pi_f}(\langle s, n \rangle) + \sup_{P^{\pi_f}(\langle s, n \rangle) \in \mathcal{P}^{\pi_f}(\langle s, n \rangle)} \sum_{s' \in S} \sum_{n' \in N} P^{\pi_f}(\langle s', n' \rangle \mid \langle s, n \rangle) \underline{V}^{\pi_f}(\langle s', n' \rangle) \\ &= C^{\pi_f}(\langle s, n \rangle) + \sup_{P^{\pi_f}(\langle s, n \rangle) \in \mathcal{P}^{\pi_f}(\langle s, n \rangle)} \sum_{s' \in S} \sum_{n' \in N} \sum_{a \in A} P^{\pi_f}(\langle s', n' \rangle \mid \langle s, n \rangle, a) \underline{V}^{\pi_f}(\langle s', n' \rangle) \\ &= C^{\pi_f}(\langle s, n \rangle) + \sup_{P^{\pi_f}(\langle s, n \rangle) \in \mathcal{P}^{\pi_f}(\langle s, n \rangle)} \sum_{a \in A} \sum_{s' \in S} \sum_{n' \in N} P^{\pi_f}(\langle s', n' \rangle \mid \langle s, n \rangle, a) \underline{V}^{\pi_f}(\langle s', n' \rangle).\end{aligned}$$

Ignoring the constant $C^{\pi_f}(\langle s, n \rangle)$, under (s, a) -rectangularity of the RPOMDP, we can continue rewriting this supremum as:

$$\begin{aligned} & \sup_{P^{\pi_f}(\langle s, n \rangle) \in \mathcal{P}^{\pi_f}(\langle s, n \rangle)} \sum_{a \in A} \sum_{s' \in S} \sum_{n' \in N} P^{\pi_f}(\langle s', n' \rangle \mid \langle s, n \rangle, a) \underline{V}^{\pi_f}(\langle s', n' \rangle) \\ &= \sum_a \sup_{P^{\pi_f}(\langle s, n \rangle, a) \in \mathcal{P}^{\pi_f}(\langle s, n \rangle, a)} \sum_{s' \in S} \sum_{n' \in N} P^{\pi_f}(\langle s', n' \rangle \mid \langle s, n \rangle, a) \underline{V}^{\pi_f}(\langle s', n' \rangle) \\ &\geq \left(\sum_a \sup_{T(s, a) \in \mathcal{T}(s, a)} \sum_{s' \in S} \sum_{n' \in N} P_T^{\pi_f}(\langle s', n' \rangle \mid \langle s, n \rangle, a) \underline{V}^{\pi_f}(\langle s', n' \rangle) \right). \end{aligned}$$

Inserting the constant $C^{\pi_f}(\langle s, n \rangle)$ again, we derive:

$$C^{\pi_f}(\langle s, n \rangle) + \sum_a \sup_{T(s, a) \in \mathcal{T}(s, a)} \sum_{s' \in S} \sum_{n' \in N} P_T^{\pi_f}(\langle s', n' \rangle \mid \langle s, n \rangle, a) \underline{V}^{\pi_f}(\langle s', n' \rangle) = \underline{V}_\star^{\pi_f}(\langle s, n \rangle).$$

Since the inequality holds for each state-memory node pair, we also have for some initial belief b_0 and initial memory node n_0 that $\underline{V}_\star^{\pi_f}(\langle b_0, n_0 \rangle) \leq \underline{V}^{\pi_f}(\langle b_0, n_0 \rangle)$. \square

Intuitively, the robust Markov chain, and thus its value function \underline{V}^{π_f} , operates under $(\langle s, n \rangle, a)$ -rectangularity, meaning nature may choose a probability distribution for each state $s \in S$, memory node $n \in N$, and action $a \in A$ independently. In the RPOMDP, and thus the associated value function $\underline{V}_\star^{\pi_f}$, nature operates under (s, a) -rectangularity, meaning it chooses probability distributions independently of the state s and action a but is restricted to choose the same probability distribution for each memory node n . The latter is more restrictive to nature, hence nature has fewer options to adversarially play against the agent. As a result, the agent's cost may be lower than when nature's choices depend on the agent's memory.

This difference in semantics may also be explicitly encoded in a partially observable stochastic game by making the agent's memory either observable or unobservable to nature [7].

B SUPERVISION POLICIES

This section elaborates on the POMDP approximations used for computing the supervision policies.

QMDP.. The Q_{MDP} algorithm [46] is an effective method to transform an optimal MDP policy to a POMDP policy by weighting the (optimal) action values Q^* of the MDP to the current belief $b \in \mathcal{B}$ in the POMDP $M \in \mathcal{M}$:

$$Q_{MDP}(b, a) = \sum_{s \in S} b(s) Q^*(s, a) = \sum_{s \in S} b(s) \left(C(s, a) + \sum_{s' \in S} T(s' \mid s, a) V_{MDP}^*(s') \right),$$

where V_{MDP}^* is the optimal value of the MDP underlying the POMDP M .

Fast-informed bound. The fast-informed bound [FIB; 24] is an approximation of the optimal value of the POMDP. It is tighter than the one given by Q_{MDP} since it includes a sum over the observation of the next state. The Q values of FIB are defined as:

$$Q_{FIB}(b, a) = \sum_{s \in S} b(s) \alpha^a(s) = \sum_{s \in S} b(s) \left(C(s, a) + \sum_{z \in Z} \min_{a' \in A} \sum_{s' \in S} T(s' \mid s, a) [z = O(s')] \alpha^{a'}(s') \right),$$

where $\alpha^a: S \rightarrow \mathbb{R}$ for each $a \in A$ is a linear function, or *alpha-vector*, updated via:

$$\alpha_{i+1}^a(s) = C(s, a) + \sum_{z \in Z} \min_{a'} \sum_{s' \in S} T(s' \mid s, a) [z = O(s')] \alpha_i^{a'}(s').$$

C TOOLS AND HYPERPARAMETERS

We use the tools Storm [26] for parsing the models and PRISM [43] to compute the RMDP values for the lower bounds in Table 1 and for robust value iteration on the Markov chain in robust policy evaluation. We build and train the RNN and the QBN using TensorFlow [1]. The RNN cell is a gated recurrent unit [GRU, 16]. Unless specified otherwise, we initialize with a concrete POMDP instance $M \in \mathcal{M}$, where the intervals of the uncertainty sets are resolved to a value in the middle of the interval $[i, j]$ given by $i+j/2$, taking into account that transitions must sum to 1. For all the experiments, the simulation batch size is set to $I = 256$, the maximum simulation length is set to $H = 200$, and we run for a maximum of 50 iterations. The RNN and QBN use an Adam optimizer [39] with a learning rate of $1 \cdot 10^{-3}$. The hidden size of the RNNs was set to $d = 16$. The experiments ran inside a Docker container on a Debian 12 machine. Our infrastructure includes an AMD Ryzen Threadripper PRO 5965WX machine with 512 GB of RAM. We train the neural networks on the CPU. The different seeds for the RNN-based methods were executed in parallel, each running on a single core. Multi-threading in the Gurobi LP solver [21] used by SCP was enabled. In our initial tests, we considered hidden sizes $d \in \{3, 16, 64\}$, batch sizes $I \in \{128, 256, 512\}$, learning rates in the range of

Table 2: Dimensions of each benchmark environment.

Instances	<i>Aircraft</i>	<i>Avoid</i>	<i>Evade</i>	<i>Intercept</i>
$ S $	13552	10225	4261	4802
$ Z $	37	6968	2202	2062
$ A $	5	4	5	4

$[1 \cdot 10^{-2}, 1 \cdot 10^{-4}]$, and different number of iterations before arriving at our final values. We used the same infrastructure and experimental setup across methods.

D NETWORK ARCHITECTURES

In this section, we provide more details on the neural network architectures. Our *post hoc* QBN approach largely follows Koul et al. [41] and Carr et al. [12], apart from differences mentioned in Section 5.4. We used a batch size of 32 for both networks during stochastic gradient descent.

D.1 QBN

Similar to prior work [12], we employ a quantized bottleneck network [QBN; 41]. It consists of an encoder $E: \hat{\mathcal{H}} \rightarrow [-1, 1]^l$ that maps the output of the RNN to a latent encoding with tanh activation, where l is the latent encoding dimension. The latent encoding is then quantized by a function $q: [-1, 1]^l \rightarrow \beta^{B_h}$, where β is the finite set of possible discrete values, for instance, $\beta = \{-1, 0, 1\}$ for three-level quantization. The *bottleneck dimension* B_h is the number of quantized neurons. Lastly, there is a decoder $D: \beta^{B_h} \rightarrow \hat{\mathcal{H}}$ to reconstruct the input given the quantized encoding. The QBN represents a function $Q: \hat{\mathcal{H}} \rightarrow \hat{\mathcal{H}}$ where $Q(\hat{h}) = D(q(E(\hat{h})))$ for all $\hat{h} \in \hat{\mathcal{H}}$. We train the QBN to minimize the reconstruction loss, *i.e.*, mean-squared error, on the RNN’s memory representations derived from the histories in \mathcal{D} . The finite set of memory nodes extracted is formed by the Cartesian product $N = \times_{B_h} \beta$, and $n = q(E(\hat{h})) \in N$ is the discrete memory representation. Therefore, the extracted FSC’s memory size $|N| = |\beta|^{B_h}$ is directly controlled by B_h and the quantization level, *i.e.*, size of the set β . Note that the quantization level can be changed to be 2-level, *i.e.*, with $B = \{-1, 1\}$ using the sign function as q , resulting in different controller sizes.

To ensure the encoder E maps to $[-1, 1]$ we use tanh activation. The gradient of this activation function is close to one around the zero input. Thus, for the 3-level quantization, we use a version \tanh_{flat} of the tanh function in the encoder that is flatter around the zero input to allow for easier learning of quantization level 0, given by [41]:

$$\tanh_{flat}(x) = 1.5 \tanh(x) + 0.5 \tanh(-3x).$$

To allow the gradient to pass through the quantization layer, we employ a simple straight-trough estimator that treats the quantization as an identity function during back-propagation [45]. The quantization activation function was provided by the Larq library [19]. The encoder and decoder use a symmetrical architecture with tanh activation. The networks were quite small. The input and output sizes of the encoder and decoder were set to the hidden size d of the RNN, with intermediate layers of sizes $8 \cdot B_h$ and $4 \cdot B_h$.

D.2 RNN

We use a Gated Recurrent Unit (GRU, Cho et al. [16]) as the RNN architecture. Although there is no clear consensus between the Long Short-Term Memory (LSTM, Hochreiter and Schmidhuber [28]) architecture and the GRU, the latter has fewer parameters than the LSTM but does have the ability to learn long-term dependencies due to the *forget gate*. The forget gate is known to combat *vanishing gradients* that occur through the variant of stochastic gradient descent employed for sequential models, known as backpropagation through time. The inputs to the RNN were put through a learnable embedding layer. We trained the RNN policy using the method in section 5.3 with a categorical cross-entropy loss implemented in TensorFlow. To prevent exploding gradients in the RNN, we use a norm-clipped gradient and orthogonal weight initialization [64] in the recurrent layer of the GRU, as recommended by Ni et al. [52]. For the policy head, we append two fully connected layers with size 32 and ReLU activation before the softmax layer mapping to the distribution over actions.

E BENCHMARK DESCRIPTIONS

In this section of the Appendix, we describe the benchmarks studied in the paper. All environments are adapted with uncertain transition functions. The grid-world environments model the probability of taking multiple steps instead of a single one for each possible moving action, to which we assign the interval $[0.1, 0.4]$. In *Aircraft*, we have two uncertainties: the probabilities of the pilot’s responsiveness and of the adversary changing direction, both mapping to the same $[0.6, 0.8]$ interval. The dimensions of the benchmarks are given in Table 2. We specify the dimensions of the grid-worlds to the same sizes as set in Carr et al. [10].

		rFSCNET				Baseline	
		QRNN	k-means++	QBN	QBN	QBN	QBN
		QMDP	QMDP	QMDP	QFIB	QMDP	QFIB
<i>Aircraft</i>	med	×	103.30	102.95	103.41	105.91	105.83
	min	×	102.03	101.91	101.88	104.66	104.60
<i>Avoid</i>	med	19.90	18.51	20.19	19.43	18.83	18.70
	min	18.62	18.16	18.57	18.53	18.39	18.35
<i>Evade</i>	med	×	37.61	37.96	38.20	36.64	36.67
	min	×	36.65	36.98	37.07	36.06	36.11
<i>Intercept</i>	med	66.00	56.20	79.71	79.51	110.47	109.36
	min	42.92	34.95	45.37	48.16	82.30	81.66

Table 3: Evaluation across multiple configurations for rFSCNET and a baseline trained on the (nominal) POMDP that resides in the middle of the uncertainty set. The values represent median (med.) and minimum (min.) robust values from the best FSCs computed of each run across 20 seeds. QRNN represents training the QBN *end-to-end*, see Section 5.4. × indicates a run failed. Bold indicates the best (med/min) performance for each environment, *i.e.*, across the rows.

E.1 Aircraft Collision Avoidance

We consider a discretized and model-uncertain version of the aircraft collision avoidance problem [40] as introduced in Cubuktepe et al. [17].

Aircraft. We follow the discretization procedure exactly and base our model on Cubuktepe et al. [17], but slightly adapt it for our expected cost formulation. The objective is to minimize the expected cost, which models avoiding a collision with an intruder aircraft while taking into account partial observability (sensor errors) and uncertainty with respect to future paths. Crashes incur an additional cost of 100 over the usual cost incurred of 1 for each action. Furthermore, the only sink states are the goal states $G \subseteq S$.

E.2 Grid-worlds

We consider the grid-worlds introduced by Junges et al. [34] but reformulate them as an expected cost (SSP) objective. All actions incur a cost of $c = 1$, with an additional penalty of $c = 100$ when in a bad state. Once again, the only sink states of the RPOMDP are the goal states $G \subseteq S$.

Avoid. The *Avoid* benchmark models a scenario where a moving agent must keep a distance from patrolling adversaries that move with uncertain speed. Additionally, its sensor yields partial information about the position of the patrolling adversaries. The agent may exploit knowledge over the predefined routes of the patrolling adversaries.

Evade. *Evade* is a scenario where a robot needs to reach a destination and evade a faster adversary. The agent has a limited range of vision but may scan the whole grid instead of moving, incurring the same cost as moving. A certain safe area is only accessible by the agent.

Intercept. *Intercept* is the opposite of *Evade* because the agent aims to meet another robot before it leaves the grid via one of two available exits. Once the target robot has exited, the agent incurs an additional penalty of $c = 100$ for each step before reaching a goal state. On top of the view radius, the agent observes a corridor in the center of the grid.

F EXTENDED EXPERIMENTAL EVALUATION

Below, the is trained in the middle of the uncertainty set, as specified in Appendix C.

F.1 Configuration Study

Due to its modularity, rFSCNET allows for different configurations that may have an effect on its performance. In Table 3, we collect median and minimum results across different configurations of rFSCNET. The combination of QMDP and k-means++ proves best, which is what is shown in the table of Table 1 in the paper. QRNN, the method that uses a QBN trained *end-to-end*, did not perform successfully on all environments. This is due to instability during training, caused by updating the QBN’s parameters with the gradients calculated from training the RNN, see Section 5.3. However, by directly encoding the clustering of the QBN into the RNN architecture during training, we observe an improvement in the median and minimum performance on the two successful runs, *Avoid* and *Intercept*, over training the QBN *post hoc*. We also show results for the baseline when trained with the two different supervision policies.

The full results in the form of boxplots are depicted in Figure 6.

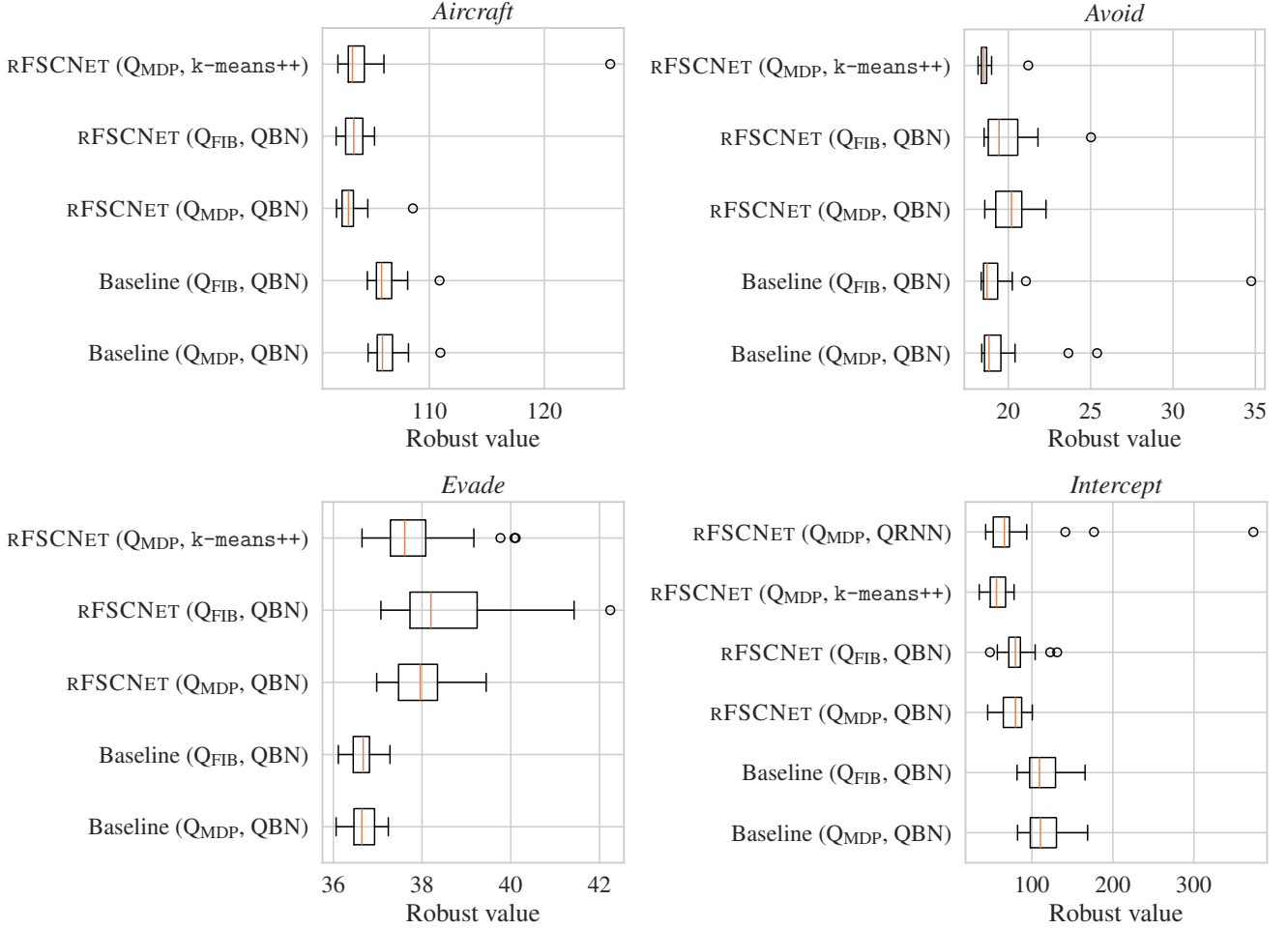


Figure 6: Comparison of the robust values between rFSCNET and a baseline trained across configurations. For *Avoid*, we plot without the run with QRNN, as it produces large outliers.

F.2 Extended Analysis on Various Memory Sizes

In this subsection, we study the memory comparison between rFSCNET and SCP in more detail. We chose *Aircraft* and *Evade*, as SCP appeared most consistent on these benchmarks. In this study, rFSCNET ran with a *post hoc* QBN and Q_{MDP} as supervision policy. We run for the maximal memory settings that we can restrict rFSCNET to when using the QBN, namely the values in the set $k \in \{3, 4, 8, 9, 16\}$, which is the size of the sets that can be found through binary $k \leq 2^{B_h}$ or ternary quantization $k \leq 3^{B_h}$, see also Appendix D.1. Figure 7 extends the right-side plot in Table 1 with statistical details. Namely, we plot the standard deviation around the median values in the heatmap and show the global min and max of each method. We observe very stable performance for our method across the various memory sizes. Both on *Aircraft* and *Evade*, SCP shows relatively stable performance across memory sizes up to $k = 9$. However, also on these benchmarks the performance drops when the required memory is set to a high level. Evidently, rFSCNET does not suffer from the same phenomenon. Furthermore, rFSCNET outperforms *Aircraft* on all memory settings and performs similarly or better than SCP on *Evade*.

F.3 Loss Comparison

Figure 8 shows the RNN and QBN losses of the baseline and rFSCNET on *Aircraft* and *Avoid*. Both runs employ a QBN and use FIB as the supervision policy. The QBN is trained individually from the RNN, *i.e.*, *post hoc*. The results show that as the RNN loss decreases, the QBN reconstruction loss increases. This tells us that it gets increasingly hard to compress the hidden states of the RNN as they get more refined. An intuition is that the RNN learns to use a larger part of \mathcal{H} to represent the hidden states as training progresses, therefore making it harder to cluster the hidden states. Alternatively, one could train the QBN *end-to-end*. However, as we elaborate in Appendix F.1, this approach suffers from instability during training and, therefore, did not successfully run on all environments.

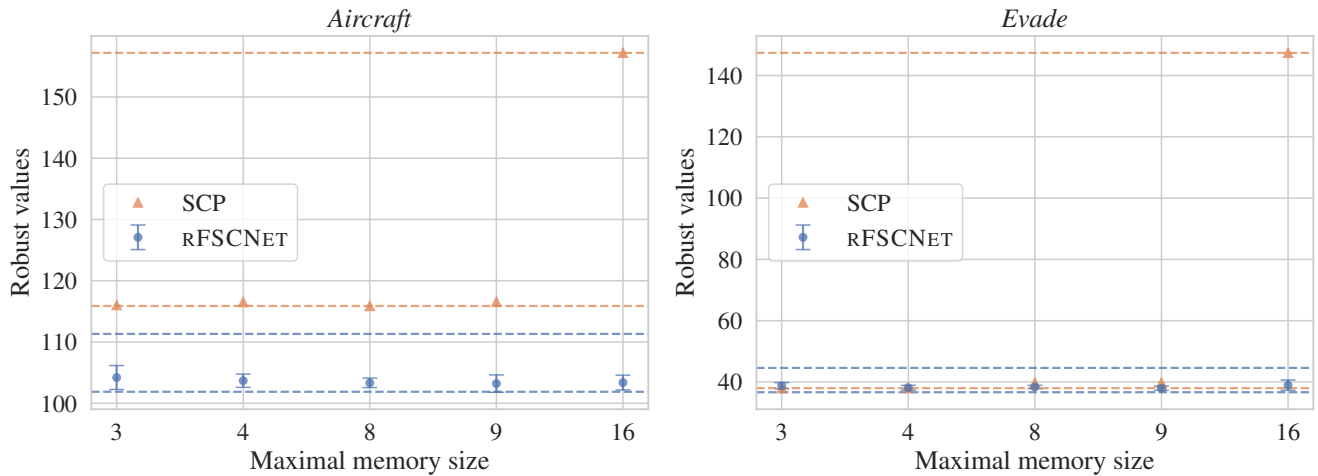


Figure 7: Comparison of the robust values between rFSCNET and SCP. For rFSCNET, the error bars depict the standard deviation, and the dotted line shows for each method the global minimum and global maximum.

G RUN TIMES

For completeness, we report the run times of each procedure for every environment in Table 4. We report the run times using a QBN trained *post hoc* and FIB, which is the most expensive configuration in terms of computations. The RNN-based run times are averaged over the 20 seeds. We would like to note that the times given for SCP are *user time* and do not account for the total *CPU time* incurred by multi-threading. For the RNN-based approach, we see that the baseline is slightly faster in every environment except for *Avoid*, as it does not execute Step 4 of our method from Section 6.2, and does not need to recompute the supervision policies as the POMDP is fixed. The run times naturally increase for larger FSCs because the Markov chain used for robust policy evaluation grows larger when the FSC has more memory nodes. Our method spends the majority of its time in its robust evaluation, executed by robust value iteration (robust dynamic programming) in PRISM. Additionally, extraction from the QBN can take longer, as $|N|$ forward passes of the RNN are required. Typically, the worse the policies found, the longer it takes to perform robust dynamic programming. By comparing the run times of the baseline to our robust method, we see that the heuristic for finding worst-case instances does increase execution time. Finally, we would like to point out that the run times for SCP could be summed for a fair comparison, as running SCP for only $k = 9$ yields much worse results than for $k = 3$.

Table 4: Average run times in seconds across 20 runs for rFSCNET and the baseline, and the *user time* of the SCP method on each environment. Thus, both run-times represent a form of user time.

	Robust ($k \leq 9$)	Baseline ($k \leq 9$)	SCP ($k = 3$)	SCP ($k = 9$)
<i>Aircraft</i>	10562.51 ± 156.03	2518.39 ± 158.76	1133.8	2169.3
<i>Avoid</i>	9987.82 ± 1209.82	12778.36 ± 1164.16	2167.9	6217.9
<i>Evade</i>	5157.85 ± 131.58	1281.85 ± 58.73	872.7	3674.1
<i>Intercept</i>	2501.95 ± 16.00	1624.33 ± 12.49	1884.9	3243.5

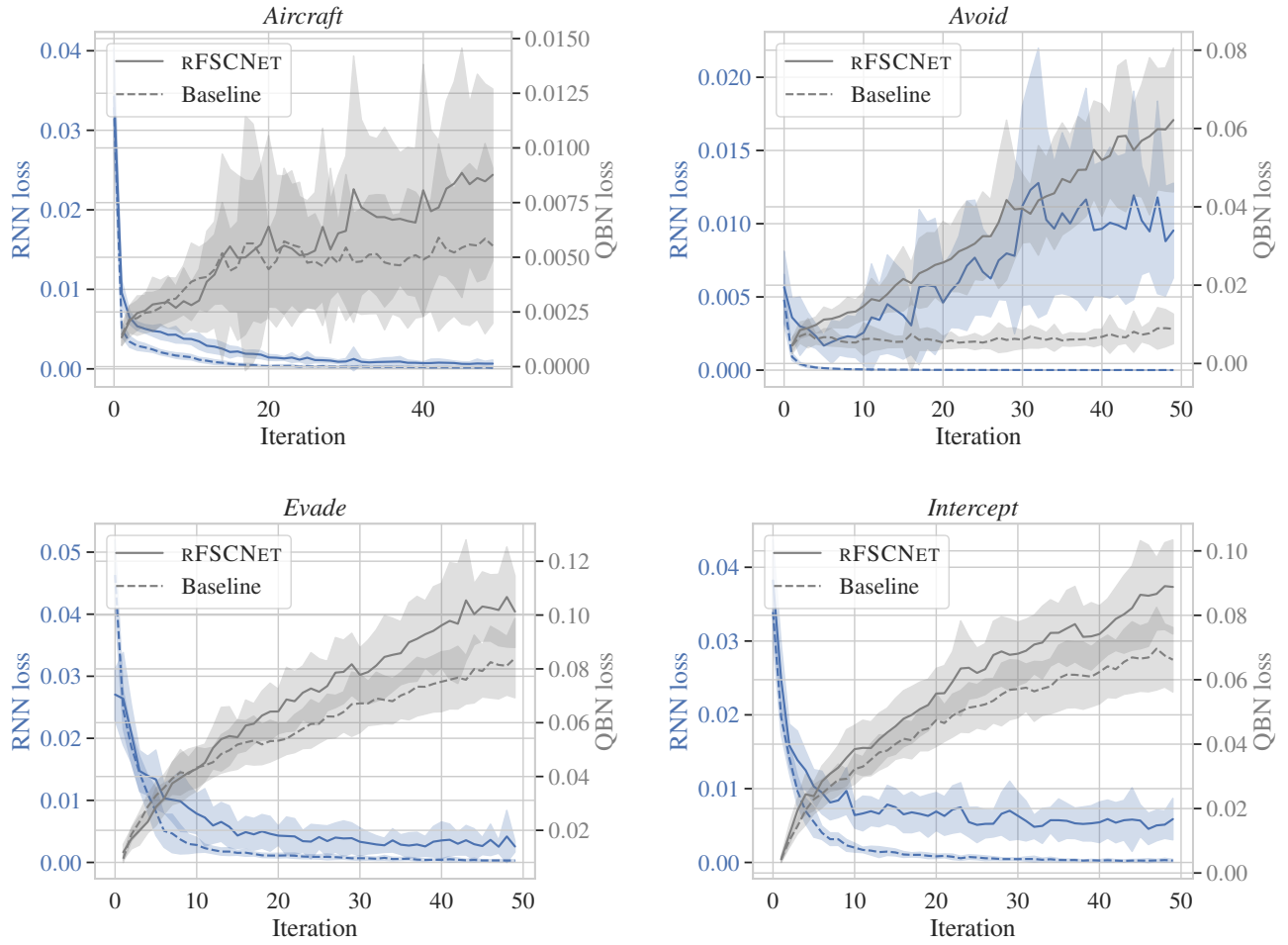


Figure 8: Comparison of RNN and QBN losses between rfSCNET and a baseline over the iterations. The line shows the mean over 20 seeds, and we plot the standard deviation around the mean for the RNN loss. On *Aircraft* and *Evade*, there is only a slight difference between the losses of the baseline and rfSCNET. On the right, on *Avoid*, a big difference is visible.